Available online at www.sciencedirect.com
SCIENCE DIRECT®
European Polymer Journal 41 (2005) 1954–1964
EUROPEAN POLYMER JOURNAL
www.elsevier.com/locate/europolj

Phase separation and structural properties of semidilute aqueous mixtures of ethyl(hydroxyethyl)cellulose and an ionic surfactant

Anna-Lena Kjøniksen [a,*], Kenneth D. Knudsen [b], Bo Nyström [a]

[a] Department of Chemistry, University of Oslo, P.O. Box 1033, Blindern, N-0315 Oslo, Norway
[b] Department of Physics, Institute for Energy Technology, P.O. Box 40, N-2027 Kjeller, Norway

Received 17 February 2005; received in revised form 16 March 2005; accepted 16 March 2005
Available online 4 May 2005

Abstract

Turbidity and small-angle neutron scattering (SANS) measurements have been carried out over an extended temperature range (10–60 °C) on thermoreversible gelling and non-gelling semidilute aqueous systems of ethyl(hydroxyethyl)cellulose (EHEC) in the presence of various amounts of sodium dodecyl sulfate (SDS). EHEC dissolved in D_2O exhibits a lower consolute solution temperature with an abrupt change of the turbidity upon heating the sample. The turbidity transformation is shifted toward higher temperatures (the cloud point temperature rises) and it becomes gradually gentler as the level of surfactant addition increases. Precision turbidity measurements demonstrate the existence of hysteresis effects when heating and cooling scans are conducted. This effect is reduced with SDS addition and disappears at a sufficiently high SDS concentration where most aggregates are disrupted. It is shown from temperature quench turbidity experiments that it takes a very long time for the temperature-induced complexes to disintegrate. The scattered intensity results from SANS at low values of the scattering vector (q) disclose that elevated temperature and low SDS concentration promote the formation of large-scale associations, and at higher levels of surfactant addition the tendency to form aggregates is suppressed. At high surfactant concentrations (8 and 16 mm), an interaction peak appears in the spectrum at intermediate values of q. For the EHEC sample with 8 mm SDS, the peak disappears at higher temperatures because of enhanced hydrophobicity of the polymer. The analysis of the SANS data for the gelling sample (EHEC with 4 mm SDS) reveals that the inhomogeneity of the gel becomes more pronounced in the post-gel region.

Keywords: Turbidity; SANS; EHEC; Gelation; Temperature effect

1. Introduction

The synergism between polymers and ionic surfactants in aqueous solutions has attracted significant interest in recent years in fundamental and applied research [1–11]. This research field is driven by the importance of mixtures of amphiphilic polymers and ionic surfactants

* Corresponding author. Tel.: +47 22 85 55 08; fax: +47 22 85 54 41.
E-mail address: a.l.kjoniksen@kjemi.uio.no (A.-L. Kjøniksen).

0014-3057/$ - see front matter © 2005 Elsevier Ltd. All rights reserved.
doi:10.1016/j.eurpolymj.2005.03.011

in a number of industrial applications including detergents, pharmaceuticals, and paints [1]. The behavior of this type of system is governed by a delicate balance between hydrophilic, hydrophobic, and ionic interactions [7]. Ethyl(hydroxyethyl)cellulose (EHEC) is one of several non-ionic amphiphilic water-soluble polymers that exhibit a lower consolute solution temperature (LCST) (demixing upon heating). This polymer is characterized by mixed hydrophobic (low amount) and hydrophilic structural units. These elements are normally unevenly distributed along the polymer backbone and the substituents may consist of shorter or longer subchains. This arrangement leads to a complex structure with an irregular distribution of hydrophobic microdomains, and the interactions between polymer chains and ionic surfactant give rise to the formation of micellar-like clusters [12] involving substituents from one or more EHEC chains. In the presence of ionic surfactants, the surfactant is bound to the polymer and this endows an apparent polyelectrolyte character to the originally non-ionic EHEC. The binding of an ionic surfactant (such as sodium dodecyl sulfate (SDS) or cetyltrimethylammonium bromide (CTAB)) to EHEC has been reported [3,10,13] to increase the cloud point temperature (CP) because of improved thermodynamic conditions of the systems.

In previous studies [2,3,10,13] of turbidity and phase separation of EHEC-surfactant systems, the principal objective was to estimate CP at various conditions and this was accomplished by slowly heating or cooling the systems and visually observing the incipient turbidity of the mixtures. Although this simple method usually yields an approximate CP it is not appropriate for a thorough description of turbidity changes and possible hysteresis effects. In this work, we will make use of a special apparatus to accurately monitor temperature-induced alterations of the turbidity in semidilute EHEC solutions (1.0 wt%) in the presence of different levels of SDS addition. By this precision cloud point analyzer instrument, we will report a detailed picture, with some novel features, of the phase separation process of the EHEC–SDS system under various conditions. This type of investigation has not been conducted on this system before. The turbidity of a material is a macroscopic phenomenon, which is linked to formation of large aggregates. To gain access to *local* structural features of the association complexes at different temperatures and levels of SDS addition, we have carried out small-angle neutron scattering (SANS) experiments on these systems. SANS measurements on EHEC-ionic surfactant solutions and gels have been reported previously [8,12], and based on these results a model has been elaborated to understand temperature-induced association and gelation in semidilute solutions of EHEC in the presence of an ionic surfactant. However, to gain a more detailed insight about the network structure of the EHEC-surfactant system at different conditions, the scattering from the polymer in the mixture has also been probed in this study by using contrast-matching conditions, adding deuterated sodium dodecyl sulfate (d-SDS) instead of SDS to EHEC. Under these conditions, the scattering length densities of the surfactant and the solvent are virtually the same, and therefore scattering from d-SDS is strongly suppressed. As a result, only the scattering from the polymer, without the contribution from the surfactant, is observed as the surfactant concentration is changed. The aim if this combined turbidity and SANS study is to characterize in detail the phase separation process and structural alterations induced by temperature and surfactant addition to a semidilute solution of EHEC. Furthermore, the SANS results for a gelling EHEC–SDS sample will be analyzed in the framework of a recent model [14–16], where the effect of heterogeneity of the system on the scattered intensity will be addressed.

2. Experimental section

2.1. Materials and solution preparation

The EHEC sample used in this study is designated DVT 89017 and was supplied by Akzo Nobel Surface Chemistry AB, Stenungsund, Sweden. For this sample the average degree of substitution of ethyl groups was DS_{ethyl} = 1.9/anhydroglucose unit, and the molar substitution of ethylene oxide groups was MS_{EO} = 1.3/anhydroglucose unit. The number average molecular weight (M_n) of this sample is approximately 80,000 and the polymer is polydisperse with a polydispersity index (M_w/M_n) of about 2. All these data have been given by the manufacturer. The anionic SDS was obtained from Fluka and the deuterated sodium dodecyl sulfate (d-SDS) was purchased from Cambridge Isotope Laboratories, Andover, USA. Both samples were used without further purification. Heavy water (D_2O) was used as solvent for the samples containing SDS, whereas for the d-SDS samples a contrast matching D_2O/H_2O mixture (91/9 vol.%) was utilized.

Dilute EHEC solutions were dialyzed against pure water for at least 1 week (until the conductivity of the expelled water showed no further decrease) to remove salt (impurity from manufacturing) and other low molecular weight components, and were thereafter freeze-dried. As the dialyzing membrane, regenerated cellulose with a molecular weight cutoff of 8000 (Spectrum Medical Industries) was utilized. After being freeze-dried, the polymer was redissolved in D_2O with the desired SDS or d-SDS concentration. The samples were prepared by weighing the components, and the solutions were allowed to stand in a refrigerator for a few days and thereafter homogenized by slow stirring at room temperature for several days. All the measurements were carried out on a semidilute (1 wt%) EHEC

sample in the presence of various amounts of SDS or d-SDS at temperatures in the interval 10–60 °C. The polymer concentration is well above the overlap concentration c^*, estimated from $c^* = 1/[\eta]$, where $[\eta]$ is the intrinsic viscosity. Depending on temperature and levels of surfactant addition, the value of c^* is in the range 0.2–0.4 wt% [11].

2.2. Turbidity experiments

The turbidities and cloud points (CP) were determined by means of an NK60-CPA cloud point analyzer from Phase Technology, Richmond, BC, Canada. This instrument makes use of a scanning diffusive light scattering technique, where a light beam (AlGaAs light source with a wavelength equal to 654 nm) is focused on the sample, to characterize phase changes of the sample with high sensitivity and accuracy. Directly above the sample, an optical system continuously monitors the scattered intensity signal (S) from the sample as it is subjected to prescribed temperature alterations. The test solution (0.15 mL) is applied onto a coated glass plate and the sample surface is covered with 0.15 mL of highly transparent silicon oil (the density of the oil is lower than that of the sample) to avoid evaporation of solvent at elevated temperatures. The temperature of the sample is probed accurately by a platinum resistance thermometer and the cooling and heating of the sample over an extended temperature range (−60 to +60 °C) is accomplished by a compact array of Peltier elements. With this arrangement, the temperature can be changed very fast (up to 30 °C/min) and the cooling or heating rate can also be set to very low values. The measured signal S from the cloud point analyzer can empirically be related to the turbidity τ, which was determined from measurements of the transmittance on a standard spectrophotometer in a 1 cm cuvette using the expression $\tau = (-1/L)\ln(I_t/I_0)$, where L is light path length of the cuvette, I_t is the transmitted light intensity, and I_0 is the incident light intensity. A direct relationship between the determined turbidity from the spectrophotometer measurements and S from the cloud point analyzer is found to be given by: $\tau = 9.0 \times 10^{-9}\ S^{3.751}$. Henceforth, all data from the cloud point analyzer will be presented in terms of turbidity. A more detailed description of the operation of the instrument and the calibration procedure has been given elsewhere [17]. The temperature at which the first deviation of the scattered intensity from the baseline occurred was taken as the cloud point of the considered sample.

2.3. Small-angle neutron scattering (SANS)

Small-angle neutron scattering (SANS) experiments were carried out on 1 wt% solutions of EHEC at different temperatures (temperature controlled to within ±0.1 °C) and in the presence of various levels of SDS addition at the SANS installation at the IFE reactor at Kjeller, Norway. The instrument is equipped with a liquid hydrogen moderator, which shifts the D_2O moderated thermal neutron spectrum (intensity maximum at approximately 1 Å) toward longer wavelengths. The wavelength was set with the aid of a velocity selector (Dornier), utilizing a high FWHM for the transmitted beam with a wavelength resolution ($\Delta\lambda/\lambda$) of 20% and maximized flux on the sample. The beam divergence was set by an input collimator (18.4 or 12.2 mm diameter) located 2.2 m from the sample, together with a sample collimator that was fixed at 4.9 mm. The detector was a 128×128 pixel, 59 cm active diameter, ^{3}He-filled RISø type detector, which is mounted on rails inside an evacuated detector chamber.

The solutions with D_2O as a solvent were filled in 2 mm Hellma quartz cuvettes, which were placed onto a copper-base for good thermal contact and mounted in the sample chamber. The chamber was evacuated to reduce air scattering.

Each complete scattering curve is composed of three independent series of measurement, using three different wavelength–distance combinations (5.1 Å/1.0 m, 5.1 Å/3.4 m, and 10.2 Å/3.4 m). By using these combinations, scattering vectors $q = (4\pi/\lambda)\sin(\theta/2)$ (where θ is the scattering angle) in the range of 0.008–0.25 Å^{-1} were covered. Standard reductions of the scattering data, including transmission corrections, were conducted by incorporating data collected from the empty cell, the beam without the cell, and the blocked-beam background. The data were transformed to an absolute scale (coherent differential cross-section $d\Sigma/d\Omega$) which is proportional to the reduced intensity $I(q)$) by calculating the normalized scattered intensity from direct beam measurements [18].

3. Results and discussion

3.1. Turbidimetry and cloud points

Before the results are presented and discussed, it may be instructive to give some fundamental aspects of the characteristic physical properties of the EHEC–SDS system. A semidilute solution of EHEC in the absence of SDS exhibits a macroscopic phase separation at sufficient heating, whereas in the presence of a moderate concentration of SDS (4 m*m*, mmolal) a thermoreversible gel is formed at elevated temperatures [9]. The gel temperature is usually somewhat lower than the corresponding cloud point temperature. The temperature-induced gelation process in semidilute EHEC solutions with an ionic surfactant can be rationalized in the framework of a model [8], where the permanent connectivity of the gel network is provided by the growing "lumps"

and the necessary swelling is generated by the electrostatic repulsions of the ionic surfactant. Each lump is formed by the loose association of polymer segments belonging to different polymer molecules, and the adsorption of ionic surfactant endows a polyelectrolyte character of the lump. Previous SANS experiments [8,12] have shown that the lump sizes increase at elevated temperature and decrease with increasing surfactant concentration. At higher concentration of the surfactant, the connectivity of the network is lost and a temperature increase only leads to a viscosification of the solution.

Fig. 1 shows the temperature dependence of the turbidity for an aqueous EHEC (1.0 wt%)–SDS (0.5 m*m*) mixture at different heating and cooling rates. The transition from a transparent to a turbid solution is sharp at this low surfactant concentration. The heating or cooling rate has no influence on the turbidity curve, but the heating and cooling cycles reveal a clear difference in the position of the curves. The results show that the heating and the subsequent cooling of the sample gives rise to a hysteresis effect. This finding indicates that the association structures formed upon heating to a high temperature do not break down directly, but rests of these structures persist over long time during the subsequent cooling cycle until low temperatures are reached. The inset plot to the left shows the time evolution of the turbidity for a sample (1 wt% EHEC–0.5 m*m* SDS) that first was quenched from 10 to 35 °C and after 12 h heated to 60 °C before it was quenched to 35 °C (35 °C is close to the point of maximum slope on the heating curve). The plot shows that after a fast (1 min) heating to 35 °C the turbidity approaches an asymptotic value after approximately 7.5 h, whereas it takes a short

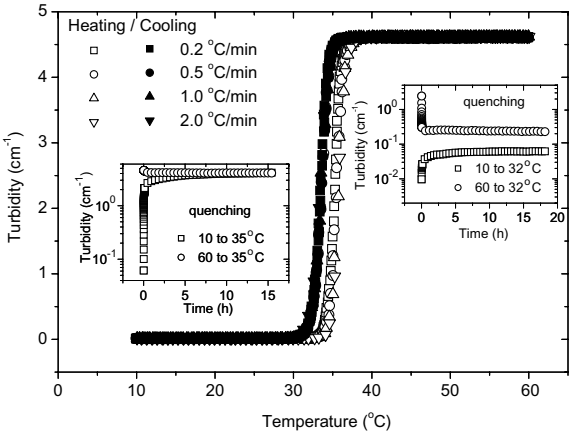

Fig. 1. Effect of temperature on the turbidity upon heating (open symbols) and subsequent cooling (solid symbols) of 1 wt% EHEC solution in the presence of 0.5 m*m* SDS. The inset plots illustrate the effects of different magnitudes of temperature quenching on the time evolution of the turbidity.

time (≈1 h) for the turbidity to reach the asymptotic value when the sample is quenched from 60 to 35 °C. This shows that it takes a long time for the association complexes to be built-up when the system is quenched from 10 to 35 °C, whereas the partial break-up at 35 °C of structures formed at 60 °C is faster. When the system is quenched to a lower temperature (32 °C), a different picture emerges (inset plot to the right). In this case, the turbidity curve obtained from quenching (10–32 °C) levels out after about 6 h, whereas the asymptotic value is approached after about 30 min when the sample is quenched from 60 to 32 °C. Furthermore, the curves do not condense onto each other. A separation of the curves is observed over long times and it is possible that they converge after times much longer than 20 h. However, we should bear in mind that this difference is small and can not be detected by a visual inspection of the sample with the naked eye. These findings demonstrate that the processes of formation and disruption of lumps operate on different time scales, and at temperatures close to CP it takes a very long time to reach the equilibrium. As will be discussed below, similar hysteresis effects are also observed at higher levels of surfactant addition.

To illustrate how the hysteresis behavior is affected by the level of surfactant addition, the heating and cooling cycles for EHEC–SDS mixtures at different SDS concentrations are depicted in Fig. 2a. At low or no surfactant addition, the samples turn turbid sharply upon a temperature increase, whereas at higher surfactant concentration the transition is gradual and shifted toward higher temperature. At moderate SDS concentrations (2 m*m* and 4 m*m*), the profile of the turbidity curves upon cooling is different, and it is obvious that large lumps exist in the samples until low temperatures have been reached. The magnitude of this hysteresis effect is reduced as the level of surfactant addition increases, and at 16 m*m* SDS the effect has disappeared. This observation shows that the large "lumps" formed at low surfactant addition and elevated temperature do not respond directly to cooling but the disruption of them is delayed, whereas at high SDS concentration the lumps are smaller (or non-existent) and easier to dissolve when the temperature is lowered.

In Fig. 2b, a quantitative illustration of the abruptness of the transition zone of the turbidity upon heating is displayed at different levels of surfactant addition by plotting the turbidity as a function of temperature in the form of a log–log plot. At surfactant concentrations up to 8 m*m*, the turbidity rise can be well represented by a power law $\tau \sim T^m$, where m is a positive number. The inset plot shows that m exhibits a strong drop at surfactant concentrations up to 2 m*m*, after which a more moderate decrease occurs. This demonstrates how the turbidity transition becomes gradually smoother as the surfactant concentration increases, suggesting

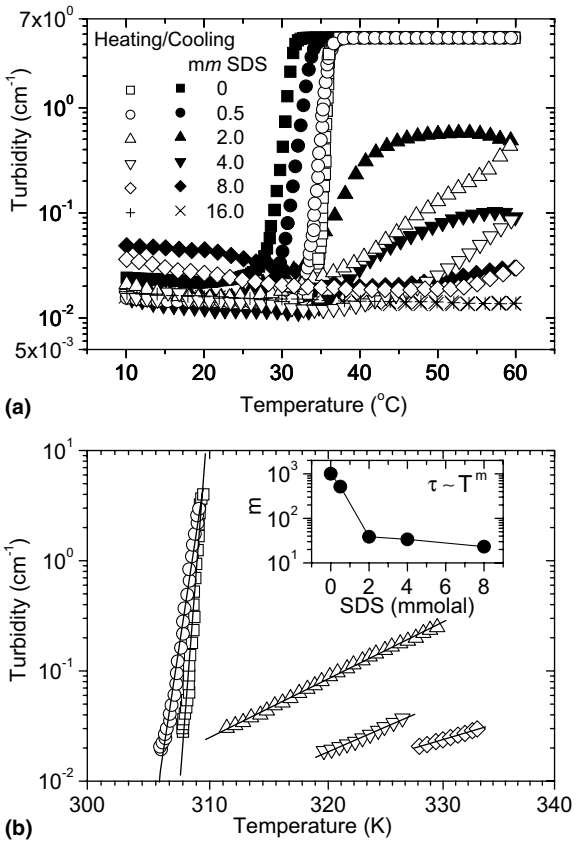

Fig. 2. (a) Temperature dependence of the turbidity upon heating (open symbols) and subsequent cooling (solid symbols) and illustration of hysteresis effects for EHEC (1 wt%)/D_2O samples in the presence of the indicated SDS concentrations. (b) Log–log plots of the turbidity versus temperature during the heating cycle at different levels of SDS addition. The data can be described by a power law relation $\tau \sim T^m$ and the effect of surfactant concentration on the power law exponent m is depicted in the inset plot.

that the temperature-induced growth of large-scale heterogeneities is reduced at higher levels of SDS addition. This behavior is ascribed to improved thermodynamic conditions (solubilization of hydrophobic microdomains) and enhanced polyelectrolyte character of the polymer.

The effect of SDS addition to 1 wt% EHEC sample on the cloud point, determined from heating scan, is depicted in Fig. 3. A salient feature is that the cloud point curve passes through a minimum at approximately 2 m*m* surfactant concentration. This effect has previously been detected by visually observing the incipient clouding of the sample (CP) [10] and the behavior was attributed to enhanced polymer-surfactant interactions as the critical aggregation concentration (cac) of the system (≈2 m*m*) was approached. The progressive surfactant binding to EHEC results in an increase in the cloud

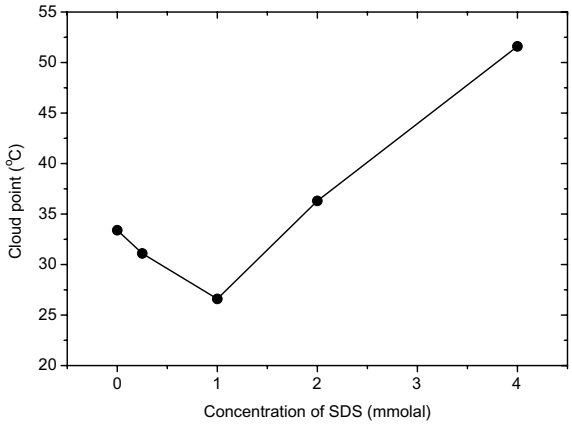

Fig. 3. Effect of SDS concentration on the cloud point determined from the heating scan of the EHEC (1 wt%)/D_2O/SDS system.

point temperature of the system; that is, the solubility of the polymer increases. The conjecture is that at higher surfactant concentrations, the hydrophobic microdomains are solubilized and the polymer becomes more hydrophilic. From a pulsed field gradient NMR investigation [4] on the EHEC–SDS system, strong interactions between the polymer and the surfactant were found and the amount of SDS bound to EHEC is roughly independent of temperature.

3.2. SANS results

Before the results are presented and discussed, some aspects concerning the analysis of the SANS data will be given. It is only the 1 wt% EHEC system with 4 m*m* SDS that forms a thermoreversible gel upon heating to 37 °C [9,19]. No gel is developed at the other surfactant concentrations, but a temperature increase induces viscosification of the solutions and the degree of turbidity of the solutions depends on the level of surfactant addition. In a semidilute polymer solution, the chains overlap and a transient network with a characteristic mesh size ξ, the screening length, is formed. In some cases, large-scale associations evolve in the solutions, giving rise to an upturn of the scattered intensity $I(q)$ at low values of q. These features can be analyzed by fitting the data to the following functional form [20,21]

$$I(q) = \frac{I_P}{q^n} + \frac{I_L}{1 + q^2\xi^2} + P \qquad (1)$$

where the first term on the right-hand side depicts the Porod scattering from large objects, and the second term is a Lorentzian (Ornstein–Zernike law) describing scattering from the polymer network. The factors I_P and I_L, the incoherent background P, and the exponent n are used as fitting parameters. The introduction of cross-links in the formation of a gel may induce effects

such as an increase of inhomogeneities, topological memory constrains, and reduction of chain mobility. The spatial, topological, and connectivity inhomogeneities that can arise may lead to the emergence of frozen inhomogeneities and non-ergodic features. For gels composed of flexible chains, the scattered intensity can be described by a sum of dynamic and static components in the form of Lorentz and squared-Lorentz functions [15,16,22]

$$I(q) = \frac{I_L}{1 + q^2\xi^2} + \frac{I_{SL}}{(1 + q^2\Xi^2)^2} + P \qquad (2)$$

where I_L and I_{SL} are factors describing the amplitudes of the dynamic and static concentration fluctuations, respectively. The parameter ξ is the dynamic correlation or screening length and Ξ is the characteristic length representing inhomogeneities. Changes in the second term on the right-hand side of Eq. (2) essentially reflect the redistribution of the polymer within the gel at large length scales.

The effect of temperature on the scattered intensity for EHEC (1 wt%) systems at different levels of SDS addition is displayed in Fig. 4. At surfactant concentrations (0 and 0.5 m*m*) below the critical aggregation concentration (cac), the upturn of the scattered intensity becomes gradually stronger as the temperature increases. The values of the power law exponent n, describing the upturn of $I(q)$ in the low q domain, are close to 4 which is a feature characteristic of Porod scattering [23] caused by smooth interfaces. This suggests that larger lumps are developed at elevated temperature and this picture is consistent with the turbidity results presented above and the scenario elaborated previously [8] from SANS studies of EHEC-surfactant systems. At moderate (2 and 4 m*m*) SDS concentrations (above cac), the rise of the scattered intensity in the low q range is less and the curves seem to level off at higher temperatures. This is probably a harbinger of that the growth of the lumps has stagnated because of binding of surfactant to the polymer. At higher levels of SDS addition (8 and 16 m*m*), the tendency of the intensity to level off is strengthened. It is evident from Fig. 4 that the amplitude of the scattered intensity falls off at low q values with decreasing temperature and increasing surfactant concentration. Since most of the scattering curves exhibit strong upturns at low q values, it is not possible to determine the size of the corresponding association structures. However, it may be instructive to consider how the amplitude of the scattering curves at a low q value is affected by temperature and surfactant concentration (see Fig. 5). The amplitude displays a strong rise with increasing temperature at low levels of surfactant addition. This trend diminishes as the surfactant concentration increases and at the highest SDS concentration virtually no temperature effect is observed. These

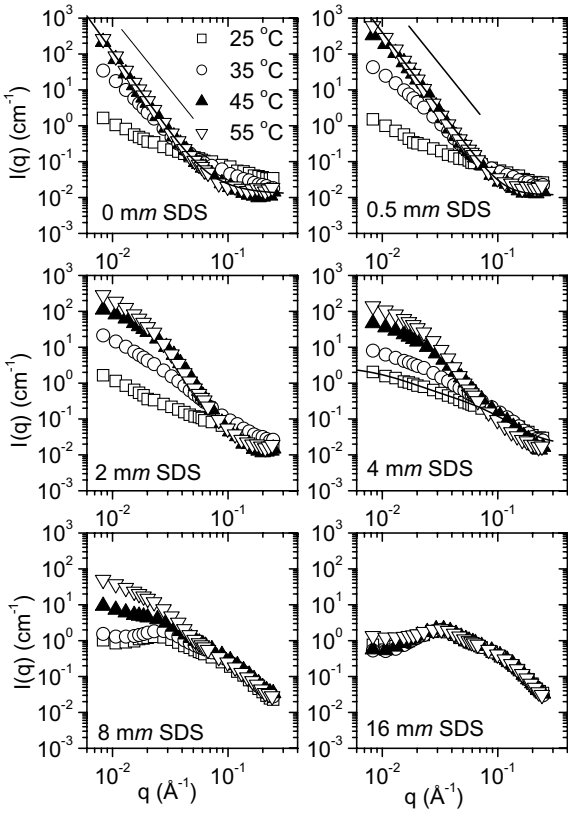

Fig. 4. SANS scattered intensity $I(q)$, plotted versus the scattering vector q at different temperatures and various levels of SDS addition for the EHEC (1 wt%)/D_2O system. Every third data point is shown. The solid line shows the Porod law ($I(q) \sim q^{-4}$). The curves represent SANS data fitted with the aid of Eq. (1) (0 and 0.5 m*m* SDS) and Eq. (2) (4 m*m* SDS).

findings are consistent with the turbidity results presented above. At lower levels of surfactant addition, the higher temperatures of the measurements are far above the values of CP for these systems and large lumps are formed, whereas at the highest SDS concentration the measurements are conducted at temperatures that are much lower than the CP of this system, and the associations are suppressed. The strong drop of the amplitude of the scattered intensity at a given high temperature with increasing SDS concentration indicates that even at an elevated temperature the multichain associations are disrupted by surfactant addition. This can be ascribed to amended thermodynamic conditions and probably electrostatic repulsive forces.

Another conspicuous feature in Fig. 4 is the interaction peak observed at intermediate q values for the higher two surfactant concentrations (8 and 16 m*m*). In Fig. 6, a direct comparison of the influence of surfactant addition on the scattered intensity at some different temperatures is displayed. We notice that the interaction peak is

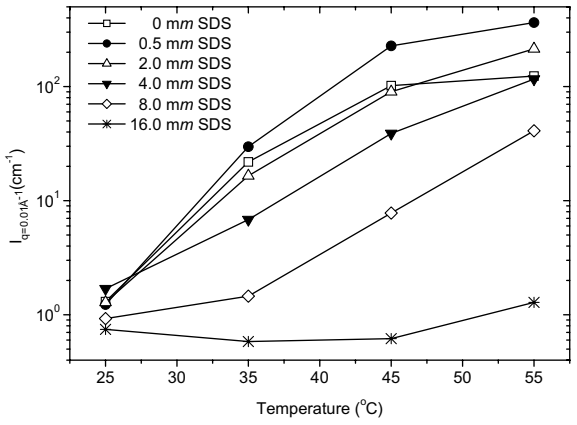

Fig. 5. Effects of temperature and SDS concentration on the amplitude of the SANS scattered intensity at a q value of 0.01 $Å^{-1}$ for EHEC (1 wt%)/D_2O samples.

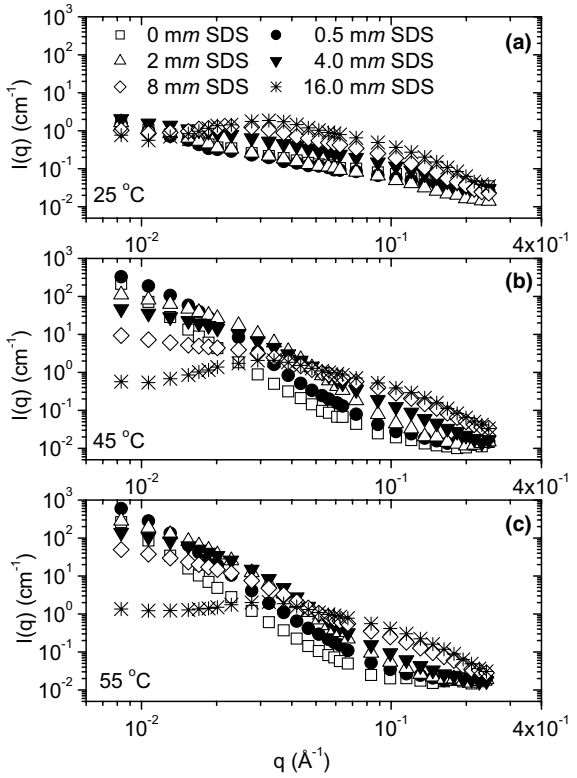

Fig. 6. Illustration of the effect of SDS addition on the SANS scattered intensity at different temperatures for EHEC (1 wt%)/D_2O samples. Every third data point is shown.

only visible at 8 m*m* and 16 m*m* SDS and the amplitude of the peak decreases with increasing temperature but the position of the maximum is almost not affected by temperature (see the discussion below). SANS is sensitive to structures with length scales of order $2\pi/q$ and the mean interaggregate distance d can be estimated from $d = 2\pi/q_{max}$, where q_{max} is the location of the maximum of the peak. For EHEC in the presence of 8 m*m* SDS, the peak disappears at the highest temperature and only a shoulder in the scattered curve is visible. This probably reflects the competition between hydrophobic and electrostatic interactions. At 55 °C (above CP) the hydrophobic associations are dominant, whereas at lower temperatures the intensity of the hydrophobic interactions are weaker and the repulsive forces are expected to play an important role for the evolution of the peak.

An interaction peak in the intermediate q domain of the SANS spectrum has been observed for many systems with polyelectrolyte character [24–31] and this behavior has been attributed to electrostatic interactions and the formation of more or less ordered arrangement of ionic structures. In theoretical approaches [14,16,32–34], the interaction peak issue has been addressed in terms of a competition between macroscopic and microscopic phase separation. In EHEC solutions without ionic surfactant, a temperature raise induces a macroscopic phase separation of the solution into a polymer-rich phase and an excess aqueous phase. Upon addition of SDS to the EHEC solution, adsorption of the surfactant to the polymer chains occurs and the phase-separation behavior of EHEC is modified because the surfactant causes fragmentation of the large regions of the polymer-rich phase into microscopic lumps (bundles of associating chains) [8] which are stabilized by the bound ionic surfactant on the surfaces of these lumps. The binding of surfactant to the lumps endows a polyelectrolyte character of the lumps. In this scenario, the microphase-separated state is made of lumps of the polymer-rich state that are kept apart from each other by the binding of ionic surfactant. At a given SDS concentration, an increase in temperature promotes growth of lumps, whereas SDS addition at a fixed temperature makes the lumps smaller. Hence, microscopic or macroscopic phase separation of the EHEC–SDS system can be tuned by changing the temperature and/or the level of surfactant addition. The prediction from the theoretical approaches is that the peak in the scattered intensity at intermediate q values signalizes the characteristic length scale of the microphase separation. The hypothesis is that the structural reorganization in connection with the transition from macroscopic to microscopic phase separation gives rise to density fluctuations that are damped on length scales larger than d and the peak in the scattering function is caused by this effect.

Since the interference peak for the EHEC–SDS system appears at SDS concentrations equal to the critical micelle concentration (8 m*m*) of SDS and above, it is crucial to check whether the peak is only a result of surfactant micelles in the bulk and not from electrostatic interactions generated by the polymer. Fig. 7 shows a

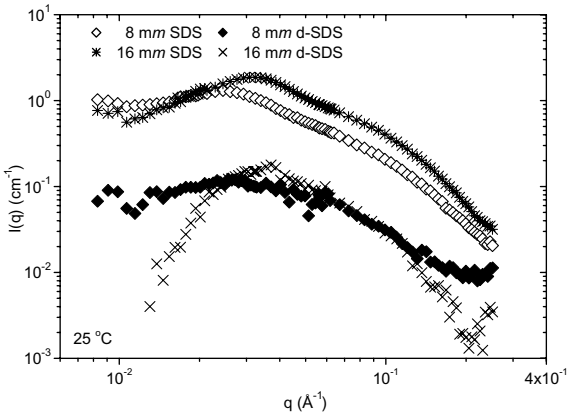

Fig. 7. A comparison of SANS data (on a log I versus log q scale) from EHEC (1 wt%)/D_2O samples in the presence of the indicated concentrations of SDS or d-SDS at 25 °C.

comparison the SANS spectra of EHEC (1 wt%) in the presence of SDS (8 and 16 m*m*) and EHEC with d-SDS, which represents contrast-matched conditions where the surfactant is "invisible" and only the polymer contributes to the signal. Although the scattered intensity is weaker with d-SDS, the profiles of the curves are similar with peaks located at practically the same positions as the corresponding peaks in the presence of SDS. However, the shoulder in the spectrum that is visible around 0.09 $Å^{-1}$ in the presence of 8 and 16 m*m* SDS cannot be detected with d-SDS. These results seem to indicate that although the free SDS micelles in the bulk significantly contribute to the scattered intensity, the peaks observed with d-SDS may represent structural arrangements, induced by electrostatic interactions of the polymer itself.

Effects of temperature and surfactant concentration on the position of the peak maximum and the average interchain distance are shown in Fig. 8. At 16 m*m* SDS, q_{max} and d are virtually independent of temperature over the studied temperature interval. The reason for this behavior is probably that in this temperature range, well below CP of the system, the thermodynamic properties and the structural rearrangements are very little influenced by a temperature change. At 8 m*m* SDS, a smaller number of larger lumps are formed and the average interchain distance d is longer than at 16 m*m*. Only two data points are displayed in the presence of 8 m*m* SDS, because at temperatures above 35 °C the interaction peak turns into a shoulder and eventually disappears at higher temperatures. The conjecture is that at temperatures approaching CP, the microphase-separated state characterized by the lumps is transformed into a macroscopic phase separation. Fig. 8b shows that the position of the maximum of the interaction peak is shifted toward higher values (i.e., the value of d decreases) as the surfactant concentration increases. At

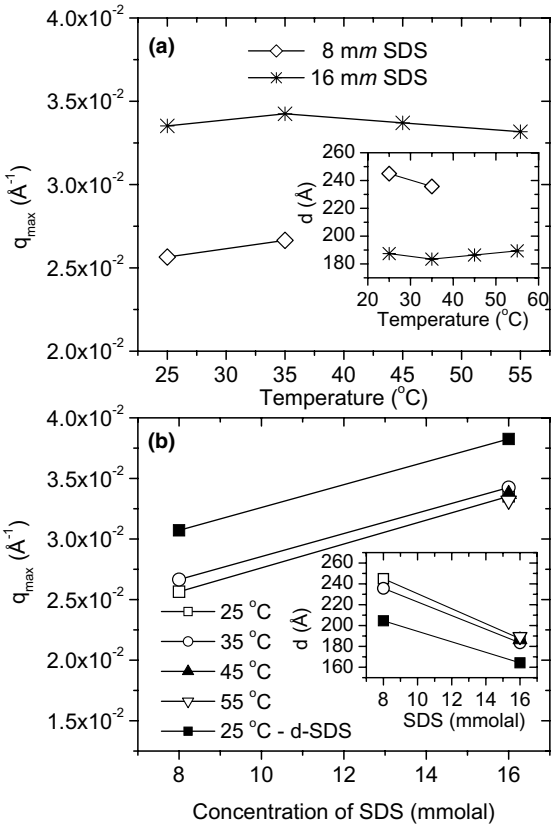

Fig. 8. Temperature and surfactant concentration dependences of q_{max} and the corresponding average interchain distance d for EHEC (1 wt%)/D_2O samples at the temperatures and surfactant concentrations indicated.

higher levels of SDS addition, a large number of fragmented lumps exist in the solution and this leads to lower values of d because the average interchain distance will decrease.

As mentioned earlier, the EHEC sample with 4 m*m* SDS forms a transparent thermoreversible gel at 37 °C [7,9], whereas no gel is formed at the other considered surfactant concentrations. The formation of a gel is governed by a delicate interplay between swelling caused by the adsorbed ionic surfactant and connectivity established by lumps or hydrophobic associations [8,12]. This prerequisite is only satisfied at certain EHEC–SDS compositions. At high levels of SDS addition, the lumps are disrupted and the connectivity is lost, while at too low surfactant concentration, the swelling is insufficient and a macroscopic phase separation is favored upon a temperature rise. The scattered intensity data at 4 m*m* SDS have been analyzed with the aid of Eq. (2) and the temperature dependencies of the fitted parameters are depicted in Fig. 9. Only scattered intensity data up to a temperature of 45 °C have been analyzed with Eq. (2) since at higher temperatures poor fits are obtained,

probably because of problems when the macroscopic phase separation is approached. The decrease of the correlation length ξ at elevated temperatures can be ascribed to the growth of the lumps and the compaction of the network. A similar trend has previously been observed [35] for the dynamic correlation length from dynamic light scattering measurements on the EHEC (1 wt%)/SDS system. The characteristic length Ξ, representing inhomogeneities of the system rises with temperature because larger lumps are formed and a more heterogeneous network evolves. It is also found (Fig. 9) that the amplitude of the static contribution of Eq. (2) increases with increasing temperature, suggesting that the frozen-in inhomogeneities of the gel network become more important at elevated temperature.

By using Eqs. (1) and (2) the scattered intensity data for various surfactant concentrations at 25 °C have been fitted and the effect of SDS addition on ξ is illustrated in Fig. 10. If the correlation length is visualized [36] as a measure of the average mesh size of the network, the observed decrease of ξ with increasing level of surfactant addition may be associated with a combination of repulsive Coulomb forces and amended thermodynamic conditions. The conjecture is that a reorganization of the network occurs from a heterogeneous network composed of bundles of close-packed chains to a homogeneous network of distributed chains when the SDS concentration increases.

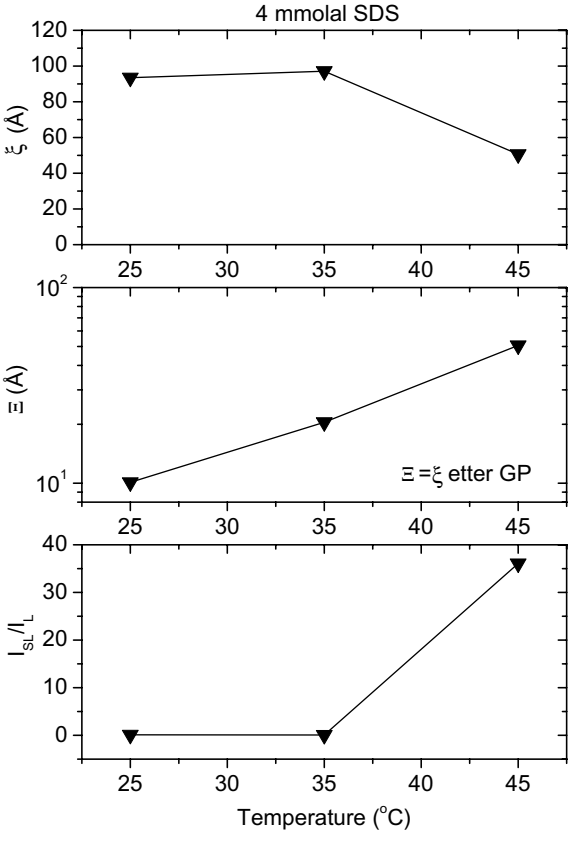

Fig. 9. Effects of temperature on the parameters obtained from Eq. (2) by fitting the SANS scattered intensity data from the gelling EHEC (1 wt%)/D_2O/SDS (4 m*m*) system.

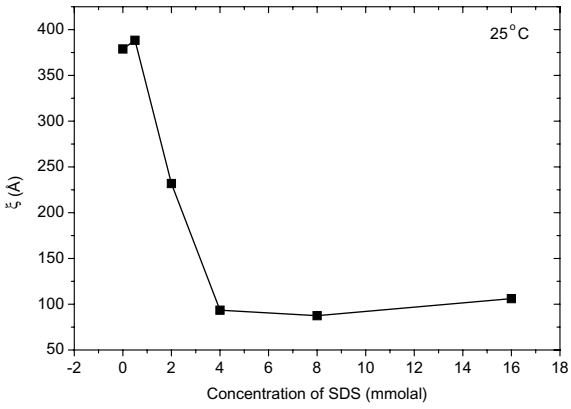

Fig. 10. Effect of SDS addition on the correlation length ξ for EHEC (1 wt%)/D_2O at a constant temperature of 25 °C. The values of have been determined by fitting the SANS data with the aid of Eq. (1) or Eq. (2).

4. Conclusions

In this work, we have provided some novel information about turbidity and SANS features in gelling and non-gelling semidilute systems of EHEC (1 wt%) in the presence of various amounts of SDS. It has been shown from turbidity measurements that the building-up and breaking-down of association complexes can be a slow process at low and moderate surfactant concentrations. An abrupt change of the turbidity with increasing temperature is observed without and at low levels of surfactant addition, whereas a gradually gentler transition is found at higher surfactant concentrations and the hysteresis effect is suppressed. The cloud point is shifted toward higher temperature as the amount of SDS increases.

The delicate interplay between macroscopic and microscopic phase separation can be affected by the temperature and the level of surfactant addition, and the accompanying structural alterations appear in the SANS results. The upturn of the scattered intensity at low q values reveals that elevated temperature and small amounts of SDS addition promotes the growth of large-scale structures. This is a prominent feature at temperatures well above the cloud point of the system. At a given high temperature, the association complexes are usually disrupted at a sufficiently high level of SDS addition. At high surfactant concentrations, an interaction

peak, characteristic for polyelectrolyte systems, was observed at intermediate q values. The position of the maximum of the peak is shifted toward higher values of q with increasing SDS concentration. At temperatures approaching the cloud point for the system, the peak turns into a shoulder and this shoulder disappears at still higher temperatures. For the gelling system, large heterogeneities evolve in the post-gel region.

Acknowledgment

B.N. and K.D.K. gratefully acknowledge support from the Norwegian Research Council through a NANOMAT Project (158550/431). K.D.K. also thanks the Marie Curie Industry Host Project (Contract No. G5TR-CT-2002-00089) for support.

References

[1] Malmsten M. Surfactants and polymers in drug delivery. Drugs and the pharmaceutical sciences, vol. 122. New York: Marcel Dekker, Inc.; 2002.
[2] Carlsson A, Karlström G, Lindman B. Characterization of the interaction between a nonionic polymer and a cationic surfactant by the Fourier transform NMR self-diffusion technique. J Phys Chem 1989;93(9):3673–7.
[3] Karlström G, Carlsson A, Lindman B. Phase diagrams of nonionic polymer-water systems: Experimental and theoretical studies of the effects of surfactants and other cosolutes. J Phys Chem 1990;94(12):5005–15.
[4] Walderhaug H, Nyström B, Hansen FK, Lindman B. Interactions of ionic surfactants with a nonionic cellulose ether in solution and in the gel state studied by pulsed field gradient NMR. J Phys Chem 1995;99(13):4672–8.
[5] Nyström B, Lindman B. Dynamic and viscoelastic properties during the thermal gelation process of a nonionic cellulose ether dissolved in water in the presence of ionic surfactants. Macromolecules 1995;28(4):967–74.
[6] Kamenka N, Zana R, Burgaud I, Lindman B. Electrical conductivity, self-diffusion, and fluorescence probe investigations of the interaction between sodium dodecyl sulfate and ethyl(hydroxyethyl)cellulose. J Phys Chem 1994;98(27):6785–9.
[7] Nyström B, Kjøniksen A-L, Lindman B. Effects of temperature, surfactant, and salt on the rheological behavior in semidilute aqueous systems of a nonionic cellulose ether. Langmuir 1996;12(13):3233–40.
[8] Cabane B, Lindell K, Engström S, Lindman B. Microphase separation in polymer + surfactant systems. Macromolecules 1996;29(9):3188–97.
[9] Kjøniksen A-L, Nyström B, Lindman B. Dynamic viscoelasticity of gelling and nongelling aqueous mixtures of ethyl(hydroxyethyl)cellulose and an ionic surfactant. Macromolecules 1998;31(6):1852–8.
[10] Lund R, Lauten RA, Nyström B, Lindman B. Linear and nonlinear viscoelasticity of semidilute aqueous mixtures of a nonionic cellulose derivative and ionic surfactants. Langmuir 2001;17(26):8001–9.
[11] Hoff E, Nyström B, Lindman B. Polymer-surfactant interactions in dilute mixtures of a nonionic cellulose derivative and an anionic surfactant. Langmuir 2001;17(1):28–34.
[12] Lindell K, Cabane B. Structures of physical gels in the EHEC-SDS-water system. Langmuir 1998;14(22):6361–70.
[13] Carlsson A, Karlström G, Lindman B. Synergistic surfactant-electrolyte effect in polymer solutions. Langmuir 1986;2(4):536–7.
[14] Onuki A. Scattering from deformed swollen gels with heterogeneities. J Phys II 1992;2(1):45–61.
[15] Horkay F, Basser PJ, Hecht A-M, Geissler E. Osmotic and SANS observations on sodium polyacrylate hydrogels in physiological salt solutions. Macromolecules 2000;33(22):8329–33.
[16] Shibayama M, Isono K, Okabe S, Karino T, Nagao M. SANS study on pressure-induced phase separation of poly(*N*-isopropylacrylamide) aqueous solutions and gels. Macromolecules 2004;37(8):2909–18.
[17] Kjøniksen A-L, Laukkanen A, Galant C, Knudsen KD, Tenhu H, Nyström B. Association in aqueous solutions of a thermoresponsive PVCL-*g*-$C_{11}EO_{42}$ copolymer. Macromolecules 2005;38(3):948–60.
[18] Wignall GD, Bates FS. Absolute calibration of small-angle neutron scattering data. J Appl Crystallogr 1987;20(1):28–40.
[19] Nyström B, Walderhaug H, Hansen FK, Lindman B. Rheological behavior during thermoreversible gelation of aqueous mixtures of ethyl(hydroxyethyl)cellulose and surfactants. Langmuir 1995;11(3):750–7.
[20] Hammouda B, Ho D, Kline S. SANS from poly(ethylene oxide)/water systems. Macromolecules 2002;35(22):8578–85.
[21] Hammouda B, Ho D, Kline S. Insight into clustering in poly(ethylene oxide) solutions. Macromolecules 2004;37(18):6932–7.
[22] Shibayama M, Suda J, Okabe S, Karino T, Okabe S, Takehisa T, et al. Structure and dynamics of poly(*N*-isopropylacrylamide)-clay nanocomposite gels. Macromolecules 2004;37(25):9606–12.
[23] Glatter O, Kratky O. Small angle X-ray scattering. London: Academic Press; 1982.
[24] Cosgrove T, White SJ, Zarbakhsh A, Heenan RK, Howe AM. Small-angle scattering studies of sodium dodecyl sulfate interactions with gelatin. 1. Langmuir 1995;11(3):744–9.
[25] Ermi BD, Amis EJ. Influence of backbone solvation on small angle neutron scattering from polyelectrolyte solutions. Macromolecules 1997;30(22):6937–42.
[26] Borsali R, Nguyen H, Pecora R. Small-angle neutron scattering and dynamic light scattering from a polyelectrolyte solution: DNA. Macromolecules 1998;31(5):1548–55.
[27] Essafi W, Lafuma F, Williams CE. Structural evidence of charge renormalization in semi-dilute solutions of highly charged polyelectrolytes. Eur Phys J B 1999;9(2):261–6.
[28] Waigh TA, Ober R, Williams CE, Galin J-C. Semidilute and concentrated solutions of a solvophobic polyelectrolyte in nonaqueous solvents. Macromolecules 2001;34(6):1973–80.

[29] Nishida K, Kaji K, Kanaya T, Shibano T. Added salt effect on the intermolecular correlation in flexible polyelectrolyte solutions: Small-angle scattering study. Macromolecules 2002;35(10):4084–9.

[30] Borsali R. In: Tripathy SK, Kumar J, Nalwa HS, editors. Handbook of polyelectrolytes and their applications, vol. 2. Los Angeles: American Scientific Publishers; 2002. p. 249 [chapter 9].

[31] Knudsen KD, Lauten RA, Kjøniksen A-L, Nyström B. Rheological and structural properties of aqueous solutions of a hydrophobically modified polyelectrolyte and its unmodified analogue. Eur Polym J 2004;40(4):721–33.

[32] Borue VY, Erukhimovich IY. A statistical theory of weakly charged polyelectrolytes: Fluctuations, equation of state and microphase separation. Macromolecules 1988;21(11):3240–9.

[33] Rabin Y, Panyukov S. Scattering profiles of charged gels: Frozen inhomogeneities, thermal fluctuations, and microphase separation. Macromolecules 1997;30(2): 301–12.

[34] Bokias G, Vasilevskaya VV, Iliopoulos I, Hourdet D, Khokhlov AR. Influence of migrating ionic groups on the solubility of polyelectrolytes: Phase behavior of ionic poly(*N*-isopropylacrylamide) copolymers in water. Macromolecules 2000;33(26):9757–63.

[35] Kjøniksen A-L, Nyström B, Lindman B. Dynamic light scattering on semidilute aqueous systems of ethyl(hydroxyethyl)cellulose. Effects of temperature, surfactant concentration, and salinity. Colloids Surf A: Physicochem Eng Aspects 1999;149(1–3):347–54.

[36] de Gennes PG. Scaling concepts in polymer physics. Ithaca: Cornell University Press; 1979.